

# Dynamics of poly(vinyl methyl ketone) thin films studied by local dielectric spectroscopy

R. Casalini,<sup>1</sup> M. Labardi,<sup>2</sup> and C. M. Roland<sup>1</sup>

<sup>1</sup>Chemistry Division, Naval Research Laboratory, Washington, DC 20375-5320, USA

<sup>2</sup>CNR-IPCF, SS Pisa, Largo Pontecorvo 3, I-56127 Pisa, Italy

(Received 5 December 2016; accepted 17 February 2017; published online 9 March 2017)

Local dielectric spectroscopy, which entails measuring the change in resonance frequency of the conducting tip of an atomic force microscope to determine the complex permittivity of a sample with high spatial (lateral) resolution, was employed to characterize the dynamics of thin films of poly(vinyl methyl ketone) (PVMK) having different substrate and top surface layers. A free surface yields the usual speeding up of the segmental dynamics, corresponding to a glass transition suppression of 6.5° for 18 nm film thickness. This result is unaffected by the presence of a glassy, compatible polymer, poly-4-vinylphenol (PVPh), between the metal substrate and the PVMK. However, covering the top surface with a thin layer of the PVPh suppresses the dynamics. The speeding up of PVMK segmental motions observed for a free surface is absent due to interfacial interactions of the PVMK with the glass layer, an effect not seen when the top layer is an incompatible polymer. *Published by AIP Publishing.* [<http://dx.doi.org/10.1063/1.4977785>]

## INTRODUCTION

Adding complexity to the unsolved problem of the glass transition is the behavior of glass-forming materials subjected to physical confinement. When the latter is on the nanoscale, the resulting enormous surface to volume ratio and the intrusion of the confining geometry on correlation length scales and, for polymers, the macromolecular coils, give rise to changed, and often anomalous, properties. One dramatic effect is on the glass transition temperature, which can be lowered or increased when a material is confined, with corresponding changes of the local or segmental dynamics.<sup>1–7</sup> The alteration of the dynamics is strongly influenced by the interface, including its rigidity and the nature of the interactions.<sup>8–12</sup> Given the potential to exploit nano-confinement for applications, understanding how confinement affects the structure and dynamics of amorphous materials has drawn much attention. However, progress requires not just further experimental characterization, but also new methods that can yield new insights.

One such method is local dielectric spectroscopy (LDS), a variation on electrostatic force microscopy<sup>13,14</sup> that combines the broad range of frequencies measured by dielectric spectroscopy with the high spatial accuracy of atomic force microscopy (AFM). LDS has been developed over the last 10 years, principally by three groups.<sup>15–22</sup> In this method, the conducting tip of an AFM is used to polarize a very small area of the sample (20–30 nm laterally). The tip is supported on a flexible cantilever, whose resonance frequency,  $f_0$ , changes on application of a potential,  $V$ , due to the electrostatic force in the approach direction,  $F_z$ , between the tip and the substrate. The most sensitive, highest resolution measurements are obtained by detection of the force gradient  $dF_z/dz$ .<sup>23</sup> This gradient is proportional to the shift of the system resonant frequency  $\Delta f$ ,

$$\Delta f/V^2 = -\frac{f_0}{2k} \frac{dF_z}{dz}, \quad (1)$$

where  $k$  is the cantilever spring constant. This frequency shift can be determined very accurately, in particular by measuring its second harmonic component,  $\Delta f_{2\omega}$ , which is not influenced by the contact potential difference between tip and sample. Both the modulus and phase are measured, yielding the sample/tip capacitance,  $C^*$ ,

$$\Delta f_{2\omega}(t) = -\frac{f_0}{4k} V_0^2 \left. \frac{\partial^2 C^*}{\partial z^2} \right| \sin(2\omega t + \delta_V), \quad (2)$$

with the phase angle  $\delta_V$  given by

$$\delta_V = \arctan \left( \frac{\partial^2 C'' / \partial z^2}{\partial^2 C' / \partial z^2} \right). \quad (3)$$

Thus, the permittivity,  $\epsilon$ , of exceedingly small samples can be obtained.

The polymer studied herein is poly(vinyl methyl ketone) (PVMK), which has a convenient glass transition temperature,  $T_g$  ( $\sim 38^\circ\text{C}$ ) just above ambient temperature. Using LDS we observe the usual effect of a thin-film geometry with an air interface, speeding up of the local segmental dynamics. However, when the free surface is coated with a compatible polymer, we find the acceleration of the motions to be suppressed. This behavior can be ascribed to the constraints arising from interactions with the second polymer, poly-4-vinylphenol (PVPh), which has a substantially higher glass transition ( $158^\circ\text{C}$ ). However, the interactions are not due to mixing of the two materials, since the PVPh is always in the glassy state. The PVMK and PVPh form hydrogen bonds, which do not require interdiffusion of the polymers. These results are quite different from that observed when the top layer is an incompatible glassy polymer, for which the thin-film dynamics are equivalent to that for a free surface.<sup>24</sup>

## EXPERIMENTAL

PVMK ( $M_w = 500$  kDa) and PVPh ( $M_w = 25$  kDa) were obtained from Aldrich and used as received. Thin films were prepared by spin coating solutions of the polymers onto aluminum-coated glass slides. The thickness of the layers was controlled by the solution concentration. The average roughness of the polymer film was about 0.25 nm. For bilayer samples, the last polymer had to be deposited from a solvent that was a non-solvent for the first polymer layer. For PVMK on PVPh, chloroform was used, while for PVPh on PVMK, the solvent was isopropanol. Before deposition of the second layer, the first was dried under nitrogen at 75 °C for about 15 min. Films were also prepared from a solution of PVMK in methylketone; the measurements (not included herein) were consistent with the results using chloroform. Both polymers are hygroscopic; thus, samples were annealed at 75 °C under nitrogen for about an hour, stored in a dry box, and then maintained in a nitrogen atmosphere during the measurements.

A Bruker Multimode 8 AFM was used for the LDS experiments. A first pass was made to measure the topographic height, with the same path retraced in lift mode (lift height  $\leq 15$  nm). During the second pass, the cantilever was oscillated at resonance (oscillation amplitude = 12 nm) with an ac voltage applied between the substrate and tip. LDS measurements were performed in the frequency modulation mode described above. The resonant frequency was tracked by a phase-locked loop controller (RHK Technology PLLPro2);  $\Delta f_{2\omega}$  and  $\delta_V$  were measured using a dual phase lock-in amplifier (Stanford Research Systems SR830DSP). Two different conductive AFM tips were used, yielding results in good agreement: One with a smaller radius ( $< 30$  nm) was a platinum-coated, doped silicon AFM cantilever (Nanosensors PP-NCLPt), having a nominal spring constant  $k = 38$  N/m, and  $f_0 = 154$  kHz. The larger radius tips had a conductive diamond coating, with nominal spring constant = 60 N/m and  $f_0 = 193$  kHz. Results from the different tips were in good agreement. The instrument was operated under a nitrogen atmosphere with controlled temperature.

Note that while LDS probes the entire thickness of the sample, the electric field is stronger at the surface, potentially amplifying its contribution to the measured response. However, if any significant difference existed between the dynamics at the film surface or nearer the substrate, there would be some broadening of the relaxation spectra, which was not observed herein. The electric field is uniform across the film area.

## RESULTS

### Calibration of sample and AFM tip

The thickness of the sample,  $h$ , is determined by removing it from a small area of the substrate by scraping with a sharp blade. The AFM in topographic mode is then used to measure the resulting change in height. Next the AFM in lift mode is used to measure the electrostatic interactions, from which the sample permittivity, the desired material property, can be extracted. This analysis requires accurate knowledge of the dimensions of the AFM tip, considered as a cone with a spherical apex. For each sample the shift in the resonance

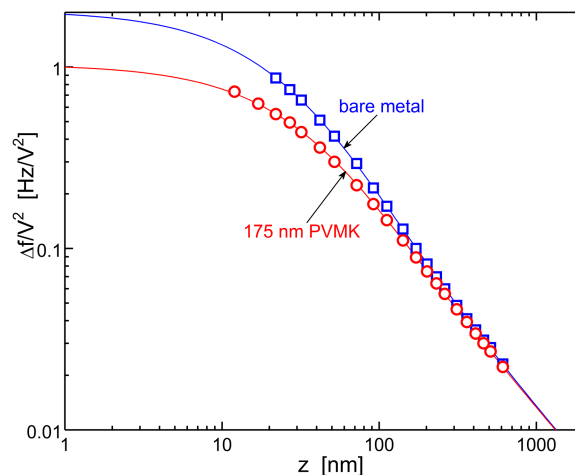


FIG. 1. Effect of changing tip distance on the resonance frequency, for the aluminum substrate bare (squares) and with a PVMK top-side coating (circles). The solid curves are fits of Eq. (4) with  $R = 100$  nm;  $\theta = 0.60$  rad;  $k = 68.9$  N/m;  $f_0 = 193$  kHz. For the polymer layer, the best-fit  $\epsilon = 10.4$ , with  $h = 175$  nm as determined using the AFM in topographic mode. The frequency was 100 Hz and the potential in the range from 2 to 9 volts. Error is less than the symbol size.

frequency is measured as a function of the distance between the tip and the sample,  $z$ . These data are fitted to a function that takes into account the contribution to the capacitance from both the apex and conical section of the tip,<sup>22</sup>

$$\Delta f_{2\omega} / V^2 = -\frac{f_0}{2k} \pi \epsilon_0 \times \left[ \frac{R}{(z + h/\epsilon)^2} - \frac{R [1 - \cos^2 \theta \sin \theta / (\pi/2 - \theta)^2]}{[z + h/\epsilon + R(1 - \sin \theta)]^2} + \frac{\sin^2 \theta_0}{(\pi/2 - \theta)^2 [z + h/\epsilon + R(1 - \sin \theta)]} \right], \quad (4)$$

in which  $\epsilon_0$  ( $= 8.85$  pF/m) is the vacuum permittivity,  $R$  the radius of curvature  $\theta$  the half-angle of the AFM conical tip, and  $k$  is the spring constant of the tip cantilever. These tip parameters are obtained by fitting Eq. (4) to data measured over an area from which the polymer has been removed, exposing the bare aluminum. The obtained values of  $R$  and  $\theta$  are consistent with SEM images of the tip. Subsequently, the measurements are repeated over an area where the sample is present, and fitting is carried out with only one adjustable parameter, the complex permittivity of the polymer. This of course is the quantity of interest; typical results are shown in Figure 1.

### Segmental relaxation of PVMK thin films

The frequency dependence of the sample permittivity  $\epsilon^*(\omega)$  is determined from the difference of phase angle measured for the bare metal substrate,  $\delta_V^m$ , and the coated substrate  $\delta_V^p$ ; i.e.,  $\Delta \delta_V = \delta_V^m - \delta_V^p$ . To describe the frequency dependence of the permittivity of the PVMK in Eq. (4), we used the Kohlrausch-William-Watts function<sup>25</sup>

$$\epsilon^*(\omega) = \Delta \epsilon \hat{L} \left[ -\frac{d \exp [-(t/\tau_K)^\beta]}{dt} \right] + \epsilon_\infty, \quad (5)$$

with  $\tau_K$ ,  $\beta$ , and  $\epsilon_\infty$  constants, and  $\hat{L}$  denotes the Laplace transform. This procedure was carried out for each sample to obtain

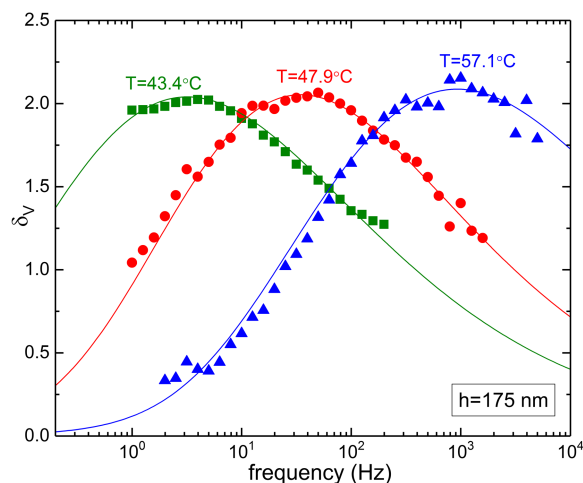


FIG. 2. The phase shift of the resonance frequency for a 175 nm thick PVMK film at the indicated temperatures. The solid line is the fit of Eqs. (4) and (5), from which the complex permittivity and hence the relaxation time are obtained. The scatter in the data points reflects the precision of the measurements.

the relaxation dispersion. Representative results are shown in Figure 2 for a 175 nm thick PVMK layer at several temperatures. Note that these peaks are shifted to higher frequency than the underlying Kohlrausch dispersion. In Figure 3 is a comparison of the peaks for PVMK films of different thicknesses (55 and 175 nm) at a common temperature. Film thickness has only a small effect on the peak breadth ( $\beta \sim 0.39 \pm 0.03$ ), not greater than the scatter in the measurements.

The relaxation times corresponding to the loss peak maximum,  $\tau$  (which is  $\sim 20\%$  larger than  $\tau_K$ ), are collected in Figure 4. The PVMK segmental dynamics become faster with decreasing film thickness. This is the usual effect for thin films having a free (air) interface. In Figure 5 we plot the temperature at which  $\tau = 5$  ms. (This is much shorter than the relaxation time at the calorimetric glass transition.) For the thinnest film the transition temperature is suppressed about 7K, with the behavior of the bulk material recovered for  $h > 170$  nm.

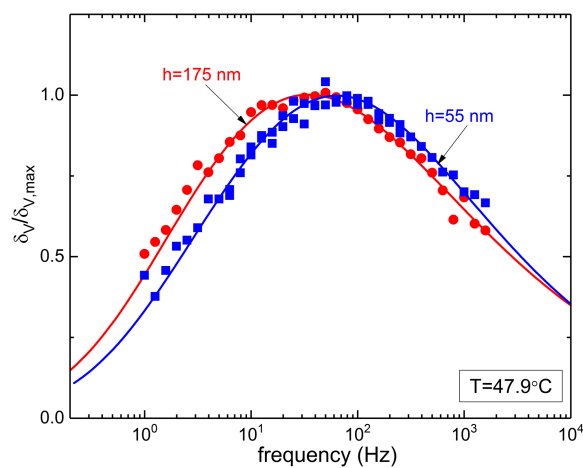


FIG. 3. The phase shift of the resonance frequency for PVMK having a film thickness equal to 55 nm (squares) and 175 nm (circles) at the indicated temperature. The solid lines are the fit of Eqs. (4) and (5). Data are normalized to unity at the peak maximum.

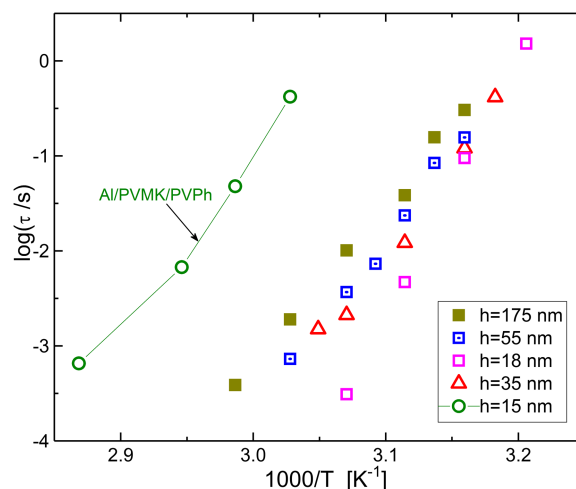


FIG. 4. Relaxation times determined from the inverse of the dielectric loss maximum as a function of temperature for various thicknesses of PVMK. The uncertainty in the ordinate values is less than the symbol size.

It has been shown that the nature of the substrate can exert an effect on the thin-film dynamics.<sup>26,27</sup> One point of contention is whether the thickness effect is greater in free-standing films than for films supported on a substrate. If this is the case, the extent of the acceleration of the dynamics would depend on the strength of the interaction with the substrate. We found previously that a weakly interacting polymer above an aluminum substrate did not affect the dynamics of thin films. Herein we investigate the case of a strongly interacting polymer (glassy PVPh) in contact with the PVMK thin film. As seen in Fig. 5, there is no apparent change in the thickness dependence of the dynamics even when the underlying substrate is a polymer that strongly interacts (H-bonds) with the substrate. The fact that the thinnest films of PVMK had equivalent dynamics, whether on the bare Al substrate or the latter coated with PVPh, indicates the predominant role of the free surface.

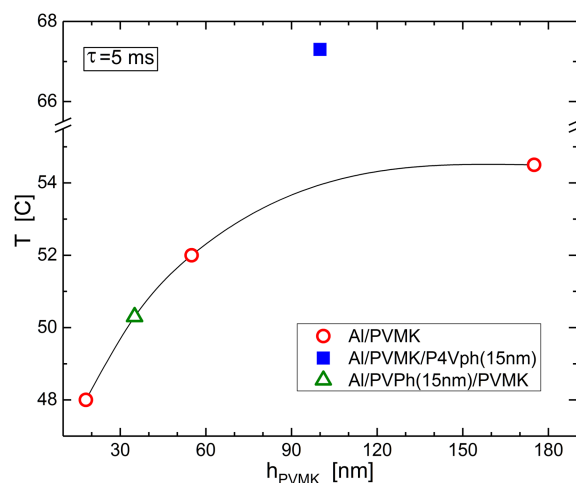


FIG. 5. Temperature at which the local segmental relaxation equals 5 ms as a function of the film thickness for PVMK with a free surface (hollow symbols) and a glassy 15 nm PVPh top-layer (square). The presence (triangle) or absence (circles) of a 15 nm PVPh layer between the Al substrate and the PVMK has no effect on the dynamics. Error bars equal the symbol size.

## Effect of loss of free surface

The speeding up of the dynamics in thin supported films is ascribed to faster dynamics at the polymer/air interface. We previously found that the dynamics of thin films of poly(vinyl acetate) (PVAc) was unaffected by a top layer of glassy poly(4-vinylpyridine), a polymer incompatible with the PVAc.<sup>24</sup> That is, replacing the free surface with a rigid material did not affect the time scale of the segmental motions, in the case of minimal interaction between the polymer layers. For miscible polymers, however, a large interfacial region can develop if both materials have segmental mobility (i.e., are above their respective glass transition temperatures). The effect on the dynamics of this interfacial mixing is very large if the two polymers have different  $T_g$ .<sup>28</sup>

Herein we consider a third possibility—the two polymers are thermodynamically miscible but one is in the glassy state, precluding interdiffusion and presumably restricting interfacial interactions. A layer of PVPh (calorimetric  $T_g$  120K higher than  $T_g$  of PVMK<sup>29</sup>) was deposited onto the top (free) surface of the PVMK. The relaxation times for PVMK in this laminate are seen in Fig. 5 to be several orders of magnitude longer than in the absence of the glassy PVPh layer, corresponding to a  $T_g$  increase of *ca.* 13K. There are two possible origins for this: interdiffusion of the miscible polymers or interactions limited to the interface. The PVPh is in the glassy state, except when being deposited from solution. However, during this deposition, the PVMK is below  $T_g$ , and unaffected by the solvent (PVMK does not absorb isopropanol). The presence of the glassy layer of PVPh is confirmed when the polymer layers are removed by scratching: the top layer of PVPh develops cracks reflecting its brittle nature (Fig. 6 top). This cracking does not occur when PVMK is scratched without the PVPh present (Fig. 6 bottom). Thus, the change in dynamics of the PVMK occurs without interdiffusion of the PVPh. It arises due to interfacial interactions, specifically hydrogen bond formation, with the PVPh. Note that although the thickness of the top layer could not be measured directly, it is estimated to be about 15 nm, based on deposition under identical conditions onto a glass slide. This thickness is very close to our limit for achieving a uniform layer. In principle  $T_g$  of the PVPh in such a thin layer could be lower than in

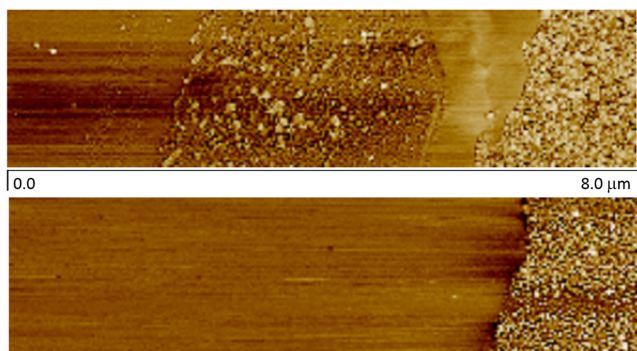


FIG. 6. Lower image: AFM of the phase measured for 175 nm PVMK film with no top layer—as prepared (left); after removal of the polymer by scraping (far right). Upper image: AFM of the phase measured for 175 nm PVMK film with 15 nm PVPh top layer—as prepared (far left); after removal of the polymer by scraping (far right); cracked, glassy PVPh surface resulting from scraping (middle).

the bulk, but the bulk value is 120K higher than  $T_g$  of the PVMK; thus, the top layer is certainly glassy over the range of temperatures used (as confirmed by the surface cracking seen in Fig. 6). For this reason, we would not expect any effect of using a thicker layer of PVPh.

## SUMMARY

The speeding up of molecular motions in thin films having a free surface is observed as well when the free surface is covered by an incompatible, glassy polymer. The repulsive nature of the interactions precludes steric or other constraints. However, when the free surface is covered with a polymer with which it strongly interacts, the enhanced mobility and a depression of  $T_g$  are absent. We find herein that this suppression of the mobility enhancement occurs even when one of the polymer layers is in the glassy state, notwithstanding the restricted interfacial mobility and absence of interdiffusion. These effects of interactions are not present when the interface is on the substrate side of the thin film; the free surface enhancement of mobility prevails.

## ACKNOWLEDGMENTS

The work at NRL was supported by the Office of Naval Research. CNR is supported in part through the Short Mobility Program No. STM2016.

- <sup>1</sup>D. D. Hsu, W. J. Xia, J. Song, and S. Keten, *ACS Macro Lett.* **5**, 481–486 (2016).
- <sup>2</sup>S. Mirigian and K. S. Schweizer, *J. Chem. Phys.* **143**, 244705 (2016).
- <sup>3</sup>M. Tarnacka, K. Kaminski, E. U. Mapesa, E. Kaminska, and M. Paluch, *Macromolecules* **49**, 6678–6686 (2016).
- <sup>4</sup>Y. Zhang, E. C. Glor, M. Li, T. Liu, K. Wahid, W. Zhang, R. A. Riggelman, and Z. Fakhraa, *J. Chem. Phys.* **145**, 114502 (2016).
- <sup>5</sup>M. D. Ediger and J. A. Forrest, *Macromolecules* **47**, 471–478 (2014).
- <sup>6</sup>V. M. Boucher, D. Cangialosi, H. Yin, A. Schonhals, A. Alegria, and J. Colmenero, *Soft Matter* **8**, 5119–5122 (2012).
- <sup>7</sup>R. D. Priestley, C. J. Ellison, L. J. Broadbelt, and J. M. Torkelson, *Science* **309**, 456–459 (2005).
- <sup>8</sup>J. DeFelice, S. T. Milner, and J. E. G. Lipson, *Macromolecules* **49**, 1822–1833 (2016).
- <sup>9</sup>W. L. Merling, J. B. Mileski, J. F. Douglas, and D. S. Simmons, *Macromolecules* **49**, 7597–7604 (2016).
- <sup>10</sup>R. J. Lang, W. L. Merling, and D. S. Simmons, *ACS Macro Lett.* **3**, 758–762 (2014).
- <sup>11</sup>Y. Guo, C. Zhang, C. Lai, R. D. Priestley, M. D'Acunzi, and G. Fytas, *ACS Nano* **5**, 5365–5373 (2011).
- <sup>12</sup>D. S. Fryer, R. D. Peters, E. J. Kim, J. E. Tomaszewski, P. F. Nealey, C. C. White, and W. L. Wu, *Macromolecules* **34**, 5627 (2001).
- <sup>13</sup>P. Girard, *Nanotechnology* **12**, 485–490 (2001).
- <sup>14</sup>D. C. Coffey and D. S. Ginger, *Nature Mater.* **5**, 735–740 (2006).
- <sup>15</sup>P. S. Crider, M. R. Majewski, J. Zhang, H. Oukris, and N. E. Israeloff, *Appl. Phys. Lett.* **91**, 013102 (2007).
- <sup>16</sup>C. Riedel, R. Arinero, P. Tordjeman, M. Ramonda, G. Leveque, G. A. Schwartz, D. G. de Oteya, A. Alegria, and J. Colmenero, *J. Appl. Phys.* **106**, 024315 (2009).
- <sup>17</sup>G. A. Schwartz, C. Riedel, R. Arinero, P. Tordjeman, A. Alegria, and J. Colmenero, *Ultramicroscopy* **111**, 1366 (2011).
- <sup>18</sup>H. K. Nguyen, D. Prevosto, M. Labardi, S. Capaccioli, M. Lucchesi, and P. A. Rolla, *Macromolecules* **44**, 6588 (2011).
- <sup>19</sup>L. A. Miccio, M. M. Kummali, G. A. Schwartz, A. Alegria, and J. Colmenero, *Ultramicroscopy* **146**, 55 (2014).
- <sup>20</sup>K. Androulaki, K. Chrissopoulou, D. Prevosto, M. Labardi, and S. H. Anastasiadis, *ACS Appl. Mater. Interfaces* **7**, 12387 (2015).
- <sup>21</sup>M. Labardi, M. Lucchesi, D. Prevosto, and S. Capaccioli, *Appl. Phys. Lett.* **108**, 182906 (2016).
- <sup>22</sup>M. Labardi, J. Barsotti, D. Prevosto, S. Capaccioli, C. M. Roland, and R. Casalini, *J. Appl. Phys.* **118**, 224104 (2015).

- <sup>23</sup>Y. Martin, C. C. Williams, and H. K. Wickramasinghe, *J. Appl. Phys.* **61**, 4723 (1987).
- <sup>24</sup>R. Casalini, D. Prevosto, M. Labardi, and C. M. Roland, *ACS Macro Lett.* **4**, 1022–1026 (2015).
- <sup>25</sup>C. M. Roland, *Viscoelastic Behavior of Rubbery Materials* (Oxford University Press, 2011).
- <sup>26</sup>S. Askar and J. M. Torkelson, *Polymer* **99**, 417–426 (2016).
- <sup>27</sup>C. M. Evans, S. Kim, C. B. Roth, R. D. Priestley, L. J. Broadbelt, and J. M. Torkelson, *Polymer* **80**, 180–187 (2015).
- <sup>28</sup>R. Casalini, L. Zhu, E. Baer, and C. M. Roland, *Polymer* **88**, 133–136 (2016).
- <sup>29</sup>H. Bourara, S. Hadjout, Z. Benabdelghani, and A. Etxeberria, *Polymer* **6**, 2752–2763 (2014).